

1 **Attenuated Total Reflection Fourier Transform Infrared Spectroscopy**  
2 **and Chemometrics for the discrimination of Animal Hair Fibers for the**  
3 **Textile Sector**

4 Christoforos Chrimatopoulos<sup>1</sup>, Maria Laura Tummino<sup>2\*</sup>, Eleftherios Iliadis<sup>1</sup>, Cinzia  
5 Tonetti<sup>2</sup>, Vasilios Sakkas<sup>1</sup>

6 <sup>1</sup>Department of Chemistry, School of Sciences, University of Ioannina, 45110 Ioannina,  
7 Greece.

8 <sup>2</sup>Institute of Intelligent Industrial Technologies and Systems for Advanced  
9 Manufacturing, National Research Council of Italy (CNR-STIIMA), Corso G. Pella 16,  
10 13900 Biella, Italy.

11 \*Corresponding author: Dr. M. L. Tummino Tel: +39 0158493043,  
12 [marialaura.tummino@cnr.it](mailto:marialaura.tummino@cnr.it)

13

14 **Abstract**

15 Analyzing the composition of animal hair fibers in textiles is crucial for ensuring the  
16 quality of yarns and fabrics made from animal hair. Among others, Fourier Transform  
17 Infrared Spectroscopy (FTIR) is a technique that identifies vibrations associated with  
18 chemical bonds, including those found in amino acid groups. Cashmere, mohair, yak,  
19 camel, alpaca, vicuña, llama and sheep hair fibers were analyzed via Attenuated Total  
20 Reflection Fourier Transform Infrared (ATR-FTIR) spectroscopy and Scanning Electron  
21 Microscopy (SEM) technique aiming the discrimination among them to identify  
22 possible commercial frauds. ATR-FTIR, being a novel approach, was coupled with  
23 chemometric tools (PLS-DA), building classification/prediction models which were  
24 cross-validated. PLS-DA models provided an excellent differentiation among animal  
25 hair of both camelids and eight animal species. In addition, the combination of ATR-  
26 FTIR and PLS-DA was used to discriminate the cashmere hair from different origins  
27 (Afghanistan, Australia, China, Iran and Mongolia). The model showed very good  
28 discrimination ability (accuracy 87%), with variance expression of 94.88 % and mean  
29 squared error of cross-validation (MSECV) of 0.1525.

30

31 **Keywords:** animal hair, textile fibers, ATR-FTIR, infrared spectroscopy, multivariate  
32 analysis, SEM

33

### 34 **Introduction**

35 Specialty animal hair fibers, such as cashmere, mohair, yak, camel, alpaca and vicuña,  
36 are valuable natural raw materials used by the fashion industry for manufacturing  
37 high-quality luxury textiles, and are distinct from sheep's wool fibers.<sup>1</sup> Although they  
38 have a very similar composition from a chemical point of view (keratin proteins), the  
39 main characteristics that confer high value to these fibers are warmth, finesse,  
40 softness, lightness, luster and, also, their rarity.<sup>2</sup> For these reasons, the cost of these  
41 fibers is high, but pretty variable depending on the specific type, and the detection of  
42 eventual adulteration is therefore essential to guarantee quality maintenance and  
43 traceability within the supply chain up to the final consumers. For instance, some  
44 features of fine yak fiber are similar to those of cashmere (i.e., in terms of the mean  
45 fiber diameter), but its price is only a quarter. Thus, the bleaching of naturally  
46 pigmented fine yak hair is highly attractive economically, potentially leading to  
47 commercial fraud.<sup>3</sup>

48 Furthermore, for example in the case of cashmere, fibers obtained in different  
49 countries have different prices in relation to their qualities.<sup>4</sup> Due to the complexity of  
50 the textile supply chain, natural fibers that are often produced in one country and  
51 subsequently processed elsewhere are more subjected to risks of label falsification.<sup>5</sup>

52 The traditional and most widely employed techniques for the identification of animal  
53 fibers in the textile sector involve microscopies. On the one hand, optical microscopy  
54 allows the study of the internal fiber structure, such as pigmentation and medulla,  
55 whereas, on the other hand, scanning electron microscopy (SEM) shows the surface  
56 morphology and the arrangement and fine structure of the cuticle cells at high  
57 resolution.<sup>2,6</sup> Further improvements in microscopy-based techniques include

58 automatization and application of deep learning and artificial intelligence,<sup>7-10</sup> and also  
59 the use of innovative equipment such as the digital holographic microscope.<sup>11</sup>

60 The investigation of the thermal behavior of fibers can be used, as well, to distinguish  
61 different animal hair, in particular, through Differential Scanning Calorimetry (DSC).  
62 Still, such analyses can be practically utilized only from a qualitative point of view.<sup>12</sup>  
63 The most important drawbacks of the techniques described above are that they are  
64 often time-consuming, subjective and operator-dependent. In order to enhance the  
65 objectivity and accuracy of the identification of animal hair fibers, even in blends,  
66 alternative methods have been proposed, analyzing protein fractions,  
67 external/internal lipids and DNA. Another method was based on specific selectivity  
68 antigen-antibody, applying monoclonal antibodies. Nevertheless, the results obtained  
69 were often affected by the influence of the chemical treatments to which the fibers  
70 have been subjected during manufacturing processes, such as bleaching,  
71 depigmentation and dyeing.<sup>13</sup>

72 Among these efforts, validated studies for the identification in mixed samples of yak,  
73 wool and cashmere fibers exploited specific molecular markers that could be  
74 unequivocally linked to individual species, bringing about an excellent qualitative and  
75 quantitative identification of cashmere, wool and yak. The procedure includes the  
76 enzymatic digestion of keratin extracted from the fibers and the peptide analysis by  
77 ultra-performance liquid chromatography – electrospray mass spectrometry (UPLC-  
78 ESI-MS). This method has become an international standard “ISO 20418-1 Textiles -  
79 Qualitative and quantitative proteomic analysis of some animal hair fibres Part 1:  
80 Peptide detection using LC-ESI-MS with protein reduction”.<sup>14,15</sup> A similar proteomic  
81 approach was also adopted for South American camelid hair fibers.<sup>16</sup> However, so far,  
82 only some types of animal hair fibers can be objectively recognized and distinguished  
83 from each other with the proteomic method and, additionally, as other techniques  
84 mentioned, it is quite expensive and destructive.

85 In recent years, spectroscopic methods coupled with chemometric analyses have been  
86 developed to overcome issues in textile material identification (both natural and  
87 synthetic), even in cases of very similar compositions.<sup>17-23</sup> Recently, Deep Neural  
88 Networks (DNN) and Support Vector Machine (SVM) machine learning techniques

89 were able to discriminate the hair of five animal species with an accuracy of more than  
90 95%.<sup>24</sup>

91 In this work, the aim is to propose a method for different animal hair fiber recognitions  
92 by Attenuated Total Reflection - Fourier Transform Infrared (ATR-FTIR) spectroscopy  
93 as a fast and practical tool, as it can be used in a non-destructive way for the analysis  
94 of various samples shaped as powders, fibers, fabrics, etc. without any pretreatment.  
95 Such analyses were assisted by chemometrics, in order to set a more and more  
96 objective methodology for the discrimination of keratin-based samples, at least for a  
97 preliminary screening in the first steps of the supply chain, when the fibers are initially  
98 provided. Indeed, it is worth specifying that spectroscopy in ATR mode can be affected  
99 by chemical modification of the sample's surface, due to its intrinsic working system  
100 based on the phenomenon of total internal reflection. While research activities  
101 demonstrate the feasibility of this method, its true significance lies in the potential  
102 reduction of operating times and quality control costs of the textile industry. Recent  
103 case studies indicate that these savings can amount to hundreds of thousands of euros  
104 per year.<sup>25,26</sup>

105 The fibers considered in this research were chosen on the basis of the taxonomic  
106 classification of animals or their geographical origin to simulate different operating  
107 scenarios.

108

## 109 **Materials and Methods**

### 110 **Sample collection and ATR-FTIR measurements**

111 Hair fibers were collected from eight different animal species belonging to six animal  
112 genera in total: *Ovis* (sheep), *Capra* (cashmere goat and Angora goat, from which  
113 mohair originates), *Bos* (yak) *Camelus* (camel), *Lama* (llama), *Vicugna* (vicuña and  
114 alpaca), where the last three genera all belong to camelids (family Camelidae). In  
115 addition, white cashmere hair samples were delivered to the laboratory from five  
116 different countries around the world (Australia, Afghanistan, China, Iran and  
117 Mongolia). The fibers were supplied by leading companies in the textile sector and

118 were stored in a glass vacuum desiccator with silica gel until analysis, to control  
119 moisture levels. Hair samples were used as provided by the suppliers without any  
120 pretreatment (e.g., cleaning with solvents)<sup>27,28</sup> in order to detect the global infrared  
121 profile of the hair. Attenuated Total Reflection - Fourier Transform Infrared (ATR-FTIR)  
122 spectroscopy analysis was performed with a diamond crystal ATR-FTIR equipment  
123 (Spectrum Two FT-IR Spectrometer adjusted with UATR Two Accessory, Perkin Elmer,  
124 Waltham, MA, USA), in a wavenumber range of 4000 to 450 cm<sup>-1</sup>, at 4 cm<sup>-1</sup> resolution  
125 with 32 scans. At the beginning and before every measurement, the diamond crystal  
126 was cleaned meticulously with isopropyl alcohol. During the conduction of the  
127 measurements, an amount of animal hair, approximately 0.3 g, was placed on the  
128 surface of the crystal (2.0 × 2.0 mm).

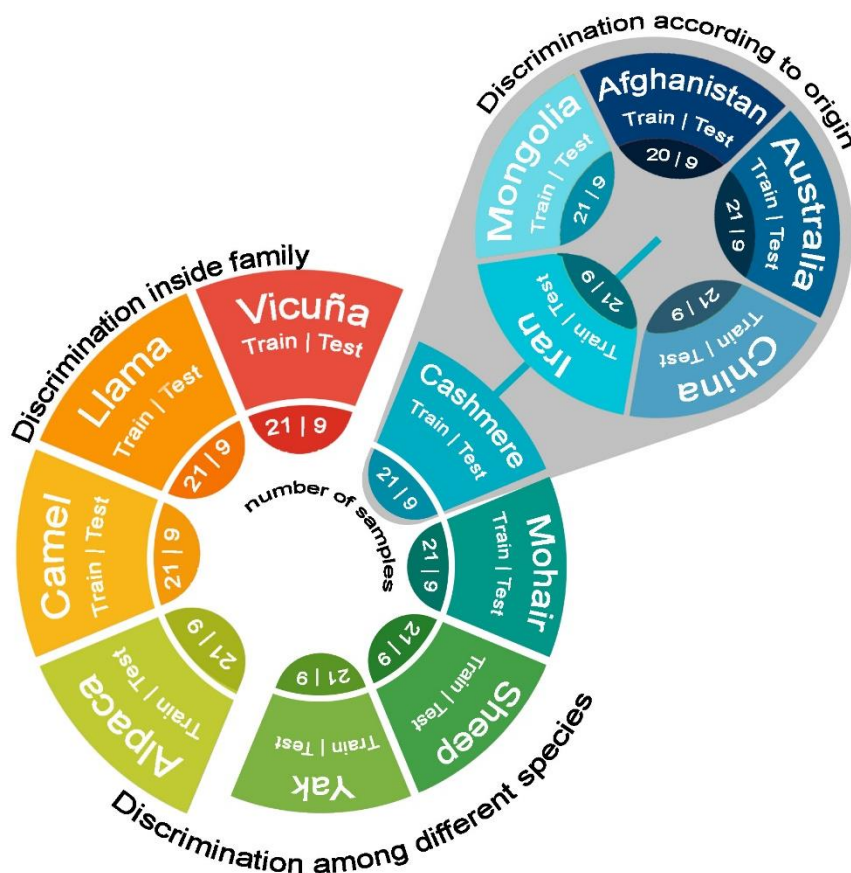
### 129 **Spectra pre-processing and data analysis**

130 The spectra pre-processing step was carried out with Spectragryph software v. 1.2.15.  
131 All animal hair spectra were baseline corrected, followed by multiplicative scatter  
132 correction (MSC). Multivariate analysis was performed with MATLAB (R2022a; The  
133 Mathworks, Natick, MA, USA), based on a previously reported work,<sup>29</sup> to build a  
134 classification with a PLS-DA model (supervised technique). In order to validate the PLS-  
135 DA model, each dataset was randomly split into a training set and a test set with a  
136 ratio of 70%:30%. The classification/prediction model was built from the training  
137 dataset of samples, and its efficiency was confirmed via the classification of the  
138 “unknown” test dataset samples. In order to avoid an overfitting effect on the  
139 upcoming classification model, 10-fold repeated stratified cross-validation (100  
140 repeats) was performed.

### 141 **Data management**

142 Following ATR-FTIR measurements, a high amount of spectra and data were obtained.  
143 The data management process for the series of studies is displayed in Figure 1. In the  
144 initial study, infrared spectra were collected for each of the eight animals  
145 (discrimination among species) to identify patterns and correlations. Then, four  
146 animals from the family of camelids were chosen to investigate in detail the  
147 discrimination ability of ATR-FTIR within the same animal family. The final deepening

148 was focused on one selected animal fiber (cashmere) from the initial eight-animal  
 149 group, studying variations and adaptations of cashmere goat hair derived from five  
 150 different geographical origins. This robust data management system ensured that the  
 151 data from these diverse sources was integrated seamlessly, allowing for  
 152 comprehensive comparisons and insightful conclusions.



153

154 **Figure 1:** Data management visualization and number of samples used (split in training and  
 155 test datasets). The colorful circle indicates the samples used for the initial discrimination  
 156 among different species. Warm-color semicircle indicates the sub-group used for the  
 157 discrimination among camelids. The small blue-color palette circle indicates the dataset used  
 158 for the discrimination of cashmere samples based on their origin.

159

160 **Morphological analyses**

161 Scanning Electron Microscopy (SEM) measurements were performed using an EVO10  
 162 instrument (Carl Zeiss Microscopy GmbH), according to the standard methods IWTO

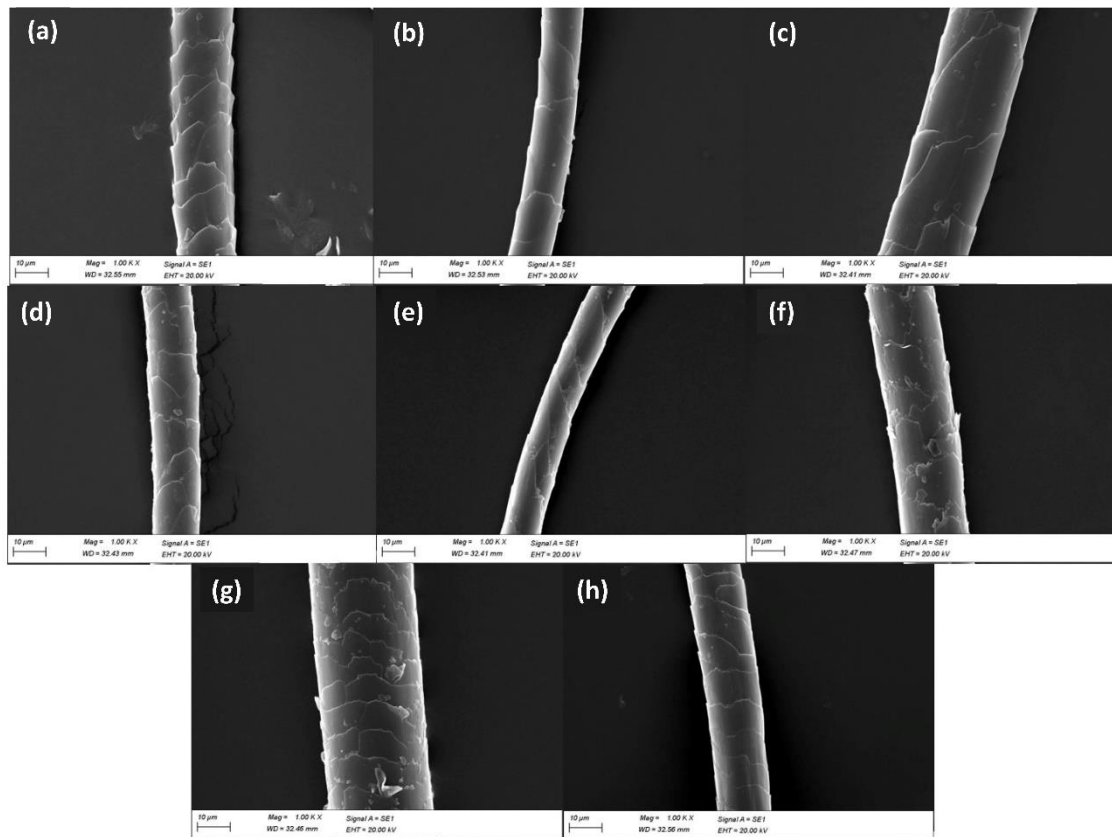
163 TM 58-00 and AATCC 20A-2017, specific for fiber analyses. The acceleration voltage  
164 was set at 20 kV. Prior to the analyses, the samples were sputter-coated with a 20 nm-  
165 thick gold layer in rarefied argon, using a Quorum Q150R ES plus Sputter Coater.

166

## 167 **Results and discussion**

### 168 **Hair fiber discrimination for different animal species and within the camelid family**

169 SEM images of the different animal fibers taken into account in this part of the study  
170 are reported in Figure 2. Generally, animal fibers are similar on the basis of their  
171 morphological features. Some distinctions are possible by carefully observing the  
172 shape and thickness of the scales and the profile of the fiber.<sup>30</sup> Due to thicker cuticle  
173 scale edges and higher scale frequency, the wool fibers are simple to identify  
174 compared to other animal fibers, assuming a significantly higher surface roughness  
175 (Figure 2a). On the contrary, the cashmere fiber scales are regular, thin with smooth  
176 surface and every scale envelopes the fiber shaft flatly and evenly. The distance  
177 between adjacent scales is large (Figure 2b). The mohair fibers exhibit an even  
178 diameter, straight fiber shaft and smooth surface. Many cuticle scales are lance-  
179 shaped, but usually, scales overlap flatly and regularly on the fiber shaft with tile  
180 shapes (Figure 2c). Finer mohair shows similar scale patterns to those of cashmere.  
181 Therefore, sometimes, it is difficult to distinguish these fibers from each other. The  
182 yak fibers have a high scale frequency and a high diameter evenness in the fiber's axial  
183 direction. Scales are thin and they encircle the fiber shaft tightly with an irregular ring-  
184 shaped pattern (Figure 2d). In the camel fibers, the scales are thin and arranged  
185 obliquely along the fiber axis. Some fine fibers have scale patterns resembling those  
186 of cashmere (Figure 2e). The alpaca fibers show a high scale frequency with less clear  
187 and ripple-crenate edges (Figure 2f). These characteristics are very similar to those of  
188 llama fibers (Figure 2g); therefore, it is not straightforward to distinguish with  
189 certainty these two kinds of fibers. Finally, the vicuña fibers have fine diameters and  
190 show high-scale frequency and characteristic axial furrows (Figure 2h).



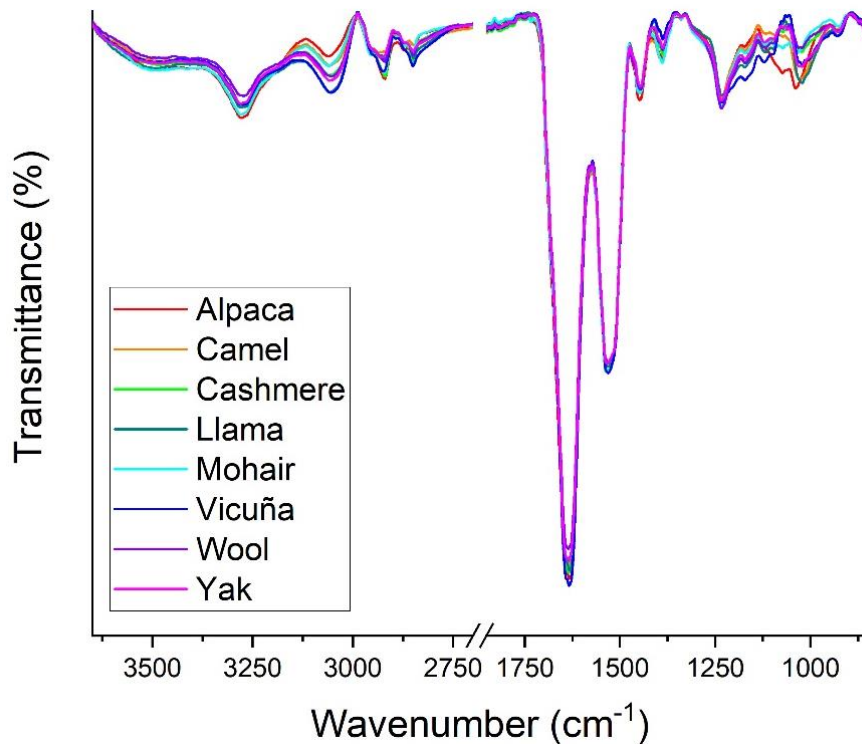
191

192 **Figure 2:** SEM images of the different animal fibers: Wool (a), Cashmere (b), Mohair (c), Yak  
 193 (d), Camel (e) Alpaca (f), Llama (g) and Vicuña (h). Scale bar: 10 μm.

194

195 In Figure 3, infrared spectra of hair fibers from the eight animal species considered are  
 196 reported.





197

198

**Figure 3:** Averaged infrared spectra of hair fibers from eight animal species.

199 The typical spectra of hair fibers consist of some macro-regions that can be  
 200 summarized as follows:

201 - The broad zone with centers at 3500 and 3275  $\text{cm}^{-1}$  due to the O-H and N-H stretching  
 202 vibrations (amide-A band)<sup>31</sup>, plus the peak at 3060  $\text{cm}^{-1}$  of Amide B;<sup>32,33</sup>

203 - The signals around 2920 and 2850  $\text{cm}^{-1}$  due to asymmetrical and symmetrical  
 204 stretching of the  $\text{CH}_2$  and  $\text{CH}_3$  groups;<sup>34-37</sup>

205 - The peaks at 1634  $\text{cm}^{-1}$  (Amide I) and at 1530  $\text{cm}^{-1}$  (Amide II) corresponding,  
 206 respectively, to C=O stretching vibration and the coupling of the N-H bending with C=N  
 207 stretching;<sup>34</sup>

208 - The complex Amide III band at 1234  $\text{cm}^{-1}$  attributed to the in-phase combination of  
 209 C-N stretching and N-H bending, with some contribution from C-C stretching and C=O  
 210 bending vibrations;<sup>38</sup>

211 - The peaks between 1200 and 1000  $\text{cm}^{-1}$  (fingerprint region) belonging to the S-O  
 212 stretching vibration band (hair keratin contains a high amount of intra- and  
 213 intermolecular disulfide bonds of cystine amino acids).<sup>23,39</sup>

214 First of all, the absence of significant absorptions around 1760-1720  $\text{cm}^{-1}$ , where the  
215 signals of esters and organic acids of lanolin can lie, is the index of a sufficient  
216 cleanness of the fibers, making the ATR-FTIR attributions mostly relatable to the  
217 inherent characteristics of the keratin-based components.<sup>40</sup> Indeed, lanolin is the  
218 wool grease that is derived from animal skin secretion.<sup>40</sup>

219 Some of the main differences among spectra can be detected by zooming in on the  
220 spectrum in the high wavenumber region (Figure S1 in Supporting Information).  
221 Between 3250 and 3150  $\text{cm}^{-1}$ , a more pronounced shoulder in llama and vicuña  
222 spectra than in other samples can be ascribed to differences in the presence of  
223 primary and secondary amide functionalities.<sup>35</sup> However, in the range 3400-3100  $\text{cm}^{-1}$ ,  
224 also residual adsorbed moisture might influence the spectral features. In the region  
225 of C-H vibration modes, the band centered at 2920  $\text{cm}^{-1}$  is particularly diverse for yak  
226 (less sharp), camel (less intense and flat) and llama (additional shoulder at 2934  $\text{cm}^{-1}$ ),  
227 while, at 2893  $\text{cm}^{-1}$ , a small peak appeared for vicuña and sheep wool. This region  
228 seems particularly affected by the sample variation, probably not only for the C-H  
229 modes, but also for the contribution of  $\text{NH}_3^+$  stretching vibrations and the specific  
230 differences in keratin composition, as already seen in the FTIR spectra acquired in Dai  
231 et al.<sup>41</sup> Moreover, between 2885 and 2825  $\text{cm}^{-1}$ , the positions of the peaks slightly  
232 varied depending on the sample type and the intensity ratio of the signals 2851/2872  
233  $\text{cm}^{-1}$  ( $\text{CH}_2/\text{CH}_3$ ) resulted in being reduced in the cases of camel and alpaca. The  
234 explanation for these discrepancies likely lies in the aminoacidic composition -creating  
235 polypeptide chains- of the animal hair deriving from different species and exemplars.<sup>42</sup>  
236 Indeed, variable combinations of alanine, arginine, aspartic acid, cysteine, glutamine,  
237 glutamic acid, histidine, leucine, lysine, methionine, serine, threonine, tyrosine and  
238 valine are usually contained in keratins.<sup>43-45</sup> Regarding the cases in which the  
239 diminishing of the  $\text{CH}_2/\text{CH}_3$  ratio happens, for instance, it is possible to hypothesize a  
240 decrement of alanine, leucine and valine that possess a methyl group with respect to  
241 other amino acids where only  $-\text{CH}_2$  are present, like glutamic acid or cysteine that are  
242 among the most abundant ones in keratins.<sup>46</sup>

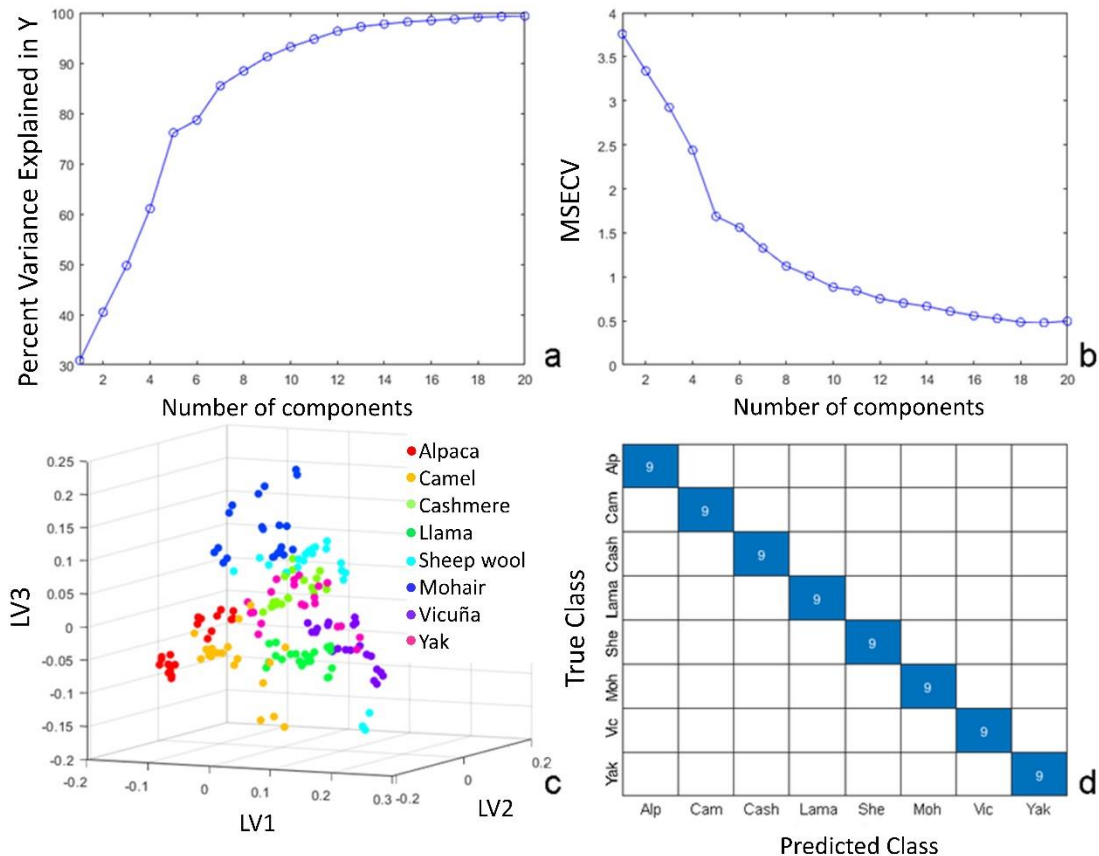
243 If the amide I and amide II bands can be considered substantially equal among the  
244 specimens, the fingerprint zone clearly highlighted other variations (Figure 3). The

245 transmittance values for vicuña, from 1233 to 1097  $\text{cm}^{-1}$ , were higher than other  
246 fibers, probably implying a difference in the secondary structures of keratin, where  $\beta$ -  
247 sheets were favored.<sup>47</sup>

248 For alpaca, the signal intensity enhancement occurred from 1138 to 966  $\text{cm}^{-1}$ ,  
249 together with a shift of the peak at 1030  $\text{cm}^{-1}$  to 1040  $\text{cm}^{-1}$ . On the contrary, the peak  
250 at about 1030  $\text{cm}^{-1}$  showed a decreased intensity in mohair, cashmere and wool  
251 samples. This latter signal is assignable to cysteine -S-sulfonate (-S-SO<sub>3</sub>-) and cysteic  
252 acid (-SO<sub>3</sub>H), whereas between 1055 and 1200  $\text{cm}^{-1}$ , cystine oxides can be  
253 detected.<sup>36,48-51</sup> Again, these discrepancies can be typical of specific amino acid  
254 presence, particularly in terms of cysteine amount and, although to a lesser extent,  
255 methionine, or an index of the oxidation state of the fibers. The oxidation state of the  
256 fibers can be related to multiple factors, namely the exposure of the animals from  
257 which the hair originates to oxidative stress sources,<sup>52-54</sup> or modifications potentially  
258 occurring in the supply chain. In this excursus, the sample that showed various  
259 peculiarities was the alpaca, which is in accordance with the literature. We suggest,  
260 indeed, that in this kind of fiber, sulfur-based and -CH<sub>2</sub>-containing amino acids, such  
261 as cysteine, are predominant at the expense of other amino acids. Atav and Türkmen  
262 have already found that Suri alpaca fibers had higher sulfur and cystine content  
263 compared with sheep wool.<sup>55</sup>

264 Given the time-expensive procedures and the necessity of experienced operators to  
265 punctually distinguish the physical-chemical characteristics of each fiber sample,  
266 multivariate analysis was applied to the infrared spectra and a PLS-DA model was built  
267 to discriminate them by a chemometric tool. In order to choose the optimum number  
268 of components to build a model expressing the maximum variance among animal  
269 species but with minimum estimated error, diagnostics and 10-fold cross-validation  
270 were performed at the training set (168 samples). As depicted in Figure 4a, a high  
271 number of components (18 latent variables, LVs) were required to achieve a variance  
272 expression of 99.10 %. Indeed, a model with 18 LVs showed the minimum mean  
273 squared error of cross-validation (MSECV, 0.4851, Figure 4b), while the LVs' increase  
274 did not add any features to the model. Figure 4c displays the score plot of the first  
275 three LVs, indicating the discrimination propensity of the model. Finally, the

276 discrimination ability of the model was evaluated with the classification of “unknown”  
 277 test dataset (72 samples). According to the confusion matrix, the 18-LVs model  
 278 succeeded with 100 % accuracy (Figure 4d), indicating very good discrimination ability.  
 279 The discrimination of alpaca, vicuña, llama, mohair and Cashmere *via* ATR-FTIR  
 280 spectroscopy and machine learning techniques has recently and successfully been  
 281 carried out in the work of Quispe et al.<sup>24</sup>

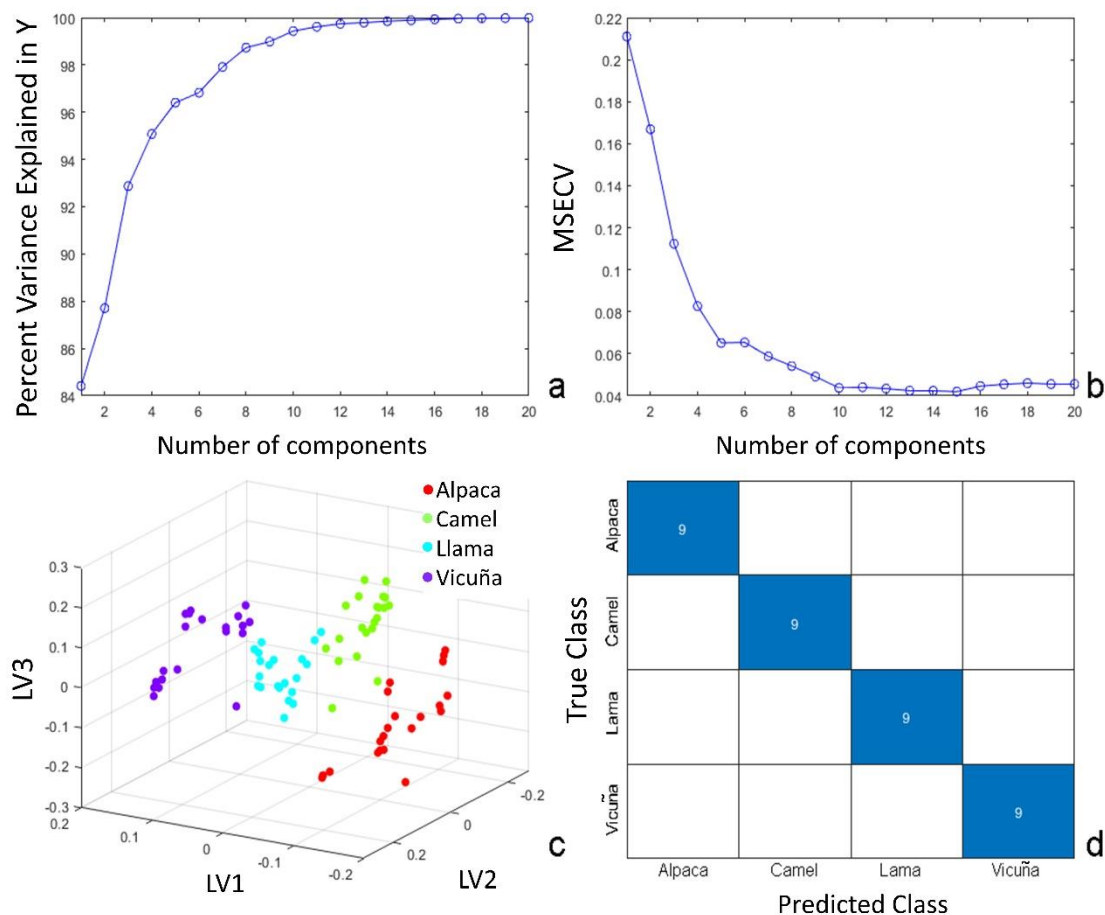


282

283 **Figure 4:** Diagnostics of the PLS-DA model among eight animal species. (a) Percentage of  
 284 variance explained in Y (groups of animal species), (b) 10-fold cross-validation of the model,  
 285 (c) score plot of the first three components (LV1, LV2, LV3) and (d) confusion matrix (using 18-  
 286 LVs) of the predicted “unknown” test dataset. In (d), Alp=alpaca, Cam=camel, Cash=cashmere,  
 287 Lama=llama, She=sheep wool, Moh=mohair, Vic= vicuña, Yak=yak. Such order is followed from  
 288 left to right in the “Predicted Class” axis and from top to bottom in the “True Class” axis.

289 However, herein because of the large number of groups that were analyzed, a high  
 290 number of components (18 LVs) were required. In order to assess the discrimination  
 291 ability of infrared spectroscopy, the study was repeated, including only the subgroup  
 292 of camelids (84 samples as the training dataset). It is evident in Figure 4c that the four

293 subgroups of camelids (alpaca, camel, llama, vicuña), at the lower part of the plot,  
 294 were slightly separated from the other groups of animals. Indeed, by reducing the  
 295 number of groups, PLS-DA could separate the four classes of camelids with only ten  
 296 LVs. According to Figure 5, a 10-LVs model was able to classify the “unknown” samples  
 297 (36 samples as test dataset) correctly with 100 % accuracy, while the expressed  
 298 variation and MSECVCV (99.43 % and 0.0437 in Figure 5a and 5b, respectively) were  
 299 much better than previously.

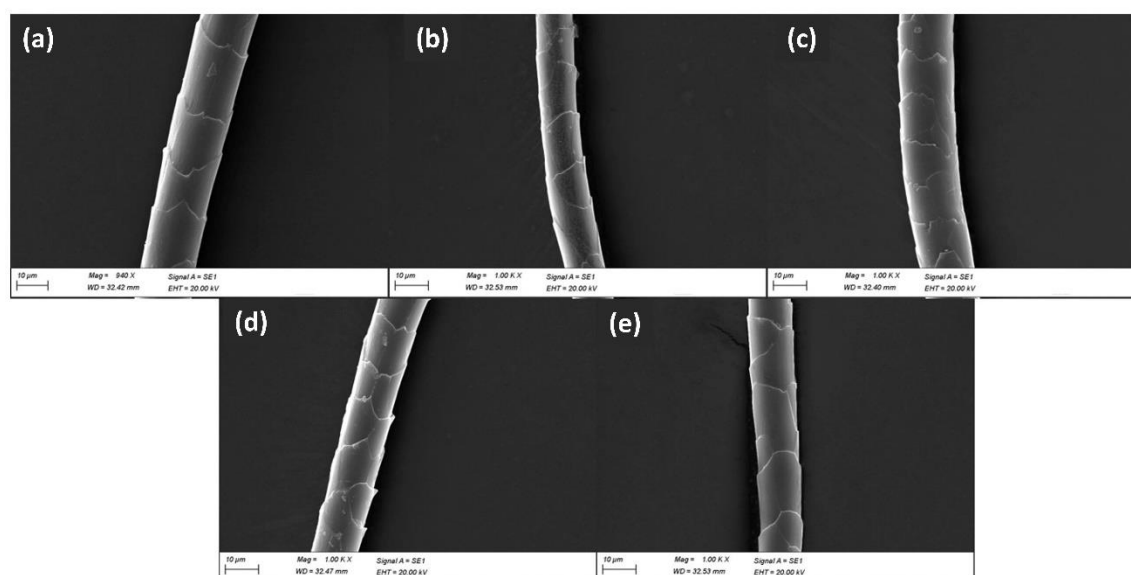


300  
 301 **Figure 5:** Diagnostics of the PLS-DA model among four camelids (alpaca, camel, llama, vicuña).  
 302 (a) Percentage of variance explained in Y (groups of camelids), (b) 10-fold cross-validation of  
 303 the model, (c) score plot of the first three components (LV1, LV2, LV3) and (d) confusion matrix  
 304 (using 10-LVs) of the predicted “unknown” test dataset.

305 These analyses confirm not only the ability of ATR-FTIR to separate animal hair from  
 306 different animal species, but also the ability to discriminate hair from animals  
 307 belonging to the same family.

308 **PLS-DA model for cashmere fibers from different origins**

309 At this point, delving further into this research, only one animal fiber type was studied,  
310 but this time, hair samples were collected from different countries (Afghanistan,  
311 Australia, China, Iran and Mongolia). It is important to point out that fibers coming  
312 from the same animal can show slight differences in morphological characteristics  
313 according to their geographical origins. However, these differences are difficult to  
314 recognize by microscopical analysis and to associate them with one origin rather than  
315 another. In Figure 6, SEM images of cashmere fibers coming from goats of different  
316 origins are reported and they are all identified as “fibers having the morphological  
317 characteristics of cashmere”.



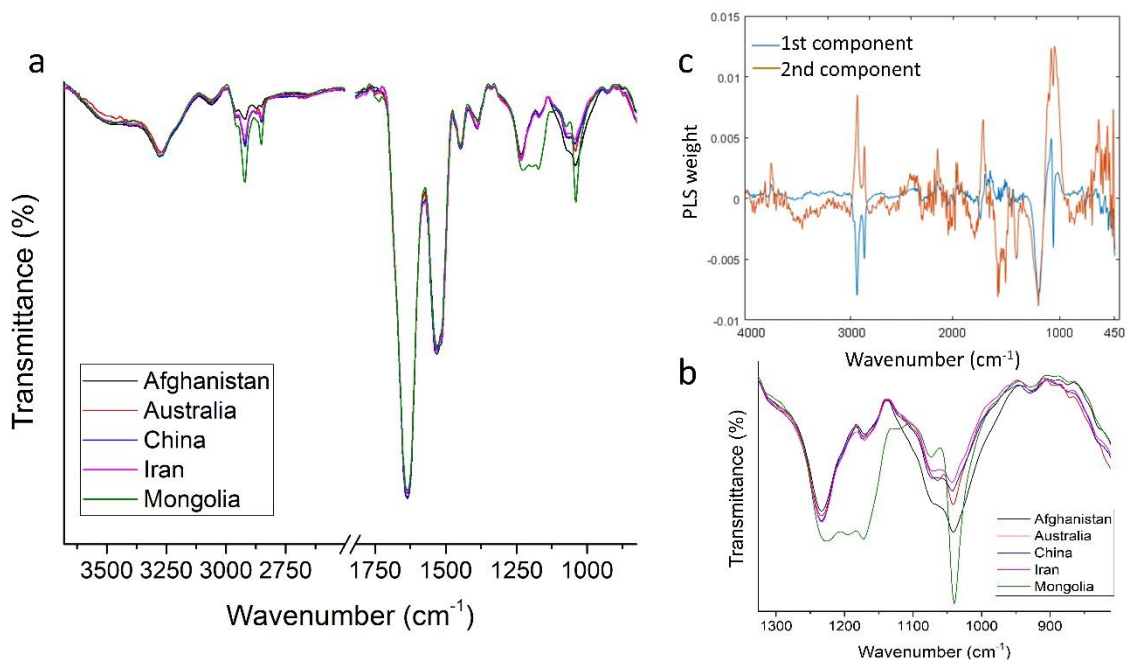
318

319 **Figure 6:** SEM images of cashmere fibers with different geographical origins: Mongolia (a),  
320 China (b), Iran (c), Afghanistan (d) and Australia (e). Scale bar: 10 µm.

321 Regarding the multivariate analysis, since it began with a maximum number of ten  
322 latent variables, 10-fold cross-validation was performed to further minimize the LVs'  
323 number (Figure S2 in Supporting Information). A compromise between a low MSEC  
324 and a minimum number of LVs was selected as an optimum prediction model without  
325 overfitting: thus, the analysis proceeded by choosing only six LVs (MSEC 0.1525) and  
326 obtaining an excellent discrimination ability.

327 The differentiation among the training dataset samples associated with the five  
328 countries of origin of the cashmere hair can be detected distinctly in the score plot of  
329 PLS-DA (Figure S3 in Supporting Information). On the one hand, Australian samples  
330 showed some variability; still, this group could be discriminated by the model. On the  
331 other hand, Mongolian samples had the best separation from the other groups.  
332 Consequently, 6-LVs PLS-DA model with an expressed variation of 94.88 % and  
333 excellent fitting ability ( $R^2 = 0.9488$ ) can be used as a suitable chemometric tool for  
334 the discrimination among the five countries of origin of the cashmere hair.

335 The analysis continued by investigating the variables associated with the  
336 discrimination. A detailed inspection of ATR-FTIR spectra (Figure 7a and 7b) together  
337 with the regression coefficients plot of the first two major components (Figure 7c)  
338 indicates all spectral characteristics from which the clustering of the samples mainly  
339 derives. As anticipated in the previous section, the detection of the peak at  $1735\text{ cm}^{-1}$   
340 in the Mongolian fibers could give an idea of a lower degree of cleanness of that  
341 sample, which can have influenced the discrimination, bringing about additional  
342 information regarding the skin secretion of the animal species. However, analyzing  
343 other more PLS-DA “sensitive” regions, between  $2980$  and  $2825\text{ cm}^{-1}$ , assigned to C-H  
344 asymmetric and symmetric stretching vibrations, the most visible event was the band  
345 intensity variation (the Mongolia sample was the most intense, whereas the  
346 Afghanistan sample showed the smallest signals). In the case of Mongolian fibers, this  
347 fact can also be associated with the superimposition of alkyl chain groups of lipids<sup>35</sup>  
348 with those of aminoacids. This hypothesis is corroborated by the presence of a  
349 broadened band comprised between  $1280$  and  $1130\text{ cm}^{-1}$  (Figure 7a and 7b), which  
350 can subtend the vibrational modes of C-O stretching, related to fatty acids.<sup>56</sup>



351

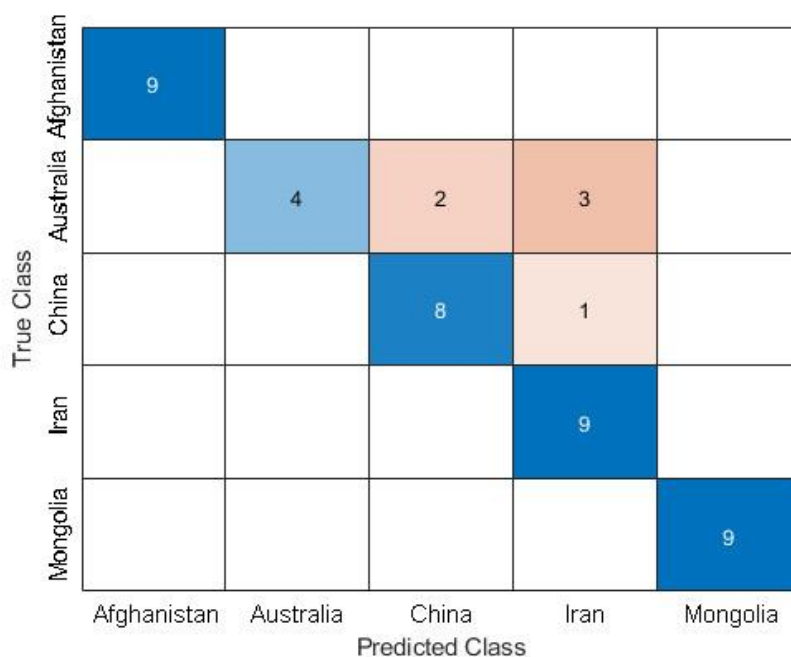
352 **Figure 7:** (a) Infrared spectra of cashmere fiber from different countries, (b) zoom of the region  
 353 1325-810 cm<sup>-1</sup> (c) PLS coefficients plot.

354 Additionally, a strong peak at 1182 cm<sup>-1</sup> (appeared in both LV1 and LV2), and two  
 355 peaks at 1056 cm<sup>-1</sup> and 1036 cm<sup>-1</sup> (the strongest among LV2's variables which were  
 356 associated with the discrimination, but in LV1 not so strong) were present in the  
 357 loading plot (Figure 7c). As already mentioned, these wavenumbers were connected  
 358 to S-O stretch vibration. More specifically, the 1200-1000 cm<sup>-1</sup> region is the infrared  
 359 window of cystine dioxide (-SO<sub>2</sub>-S-) (1182 cm<sup>-1</sup>), cystine monoxide (-SO-S-) (1056 cm<sup>-1</sup>)  
 360 and cysteic acid (-SO<sub>3</sub>H) (1036 cm<sup>-1</sup>) vibrations.<sup>49-51</sup> Looking at Figure 7b, the most  
 361 diverse band centered at about 1040 cm<sup>-1</sup> was that from Afghanistan, with its stronger  
 362 intensity. The differences observed in spectra of cashmere fibers could be correlated  
 363 with their different amino acid composition, in turn, linked with the origin and the diet  
 364 (grazing, administration of feeds, use of protected proteins) and also by the energy  
 365 intake.<sup>57</sup> Glycine, phenylalanine, serine, and tyrosine content has been reported to be  
 366 affected by the country of origin; alanine, histidine, isoleucine, proline, valine, aspartic  
 367 acid and phenylalanine levels depend on the energy nutrition and management.<sup>57</sup>

368 Multivariate analysis was ended by utilizing the developed 6-LVs PLS-DA model to  
 369 assess the test dataset samples of cashmere hair indicated as "unknown" for the  
 370 model. The confusion matrix of the test dataset is reported in Figure 8. The accuracy



371 of the model was 86.67 %, which indicates an extensive classification of the  
 372 “unknown” country of origin of the samples. Australian cashmere hair was the group  
 373 with the highest misclassification capacity, due to the fact that five out of nine  
 374 “unknown” samples were classified elsewhere. Overall, only 6 out of the total 45  
 375 samples of the test dataset were misclassified, giving the model sensitivities and  
 376 specificities presented in Table 1. These results demonstrate that ATR-FTIR coupled  
 377 with PLS-DA could satisfactorily discriminate the cashmere hair samples from different  
 378 origins.



379

380 **Figure 8:** Confusion matrix of the cashmere hair origin predictive PLS model.

381

382 **Table 1:** Sensitivity and specificity of country origin of cashmere hair.

Country origin	Sensitivity	Specificity
Afghanistan	1	1
Australia	0.44	1
China	0.89	0.94
Iran	1	0.89
Mongolia	1	1

383

## 384 **Conclusions and perspectives**

385 In summary, our study represents a significant advancement in the field of animal hair  
386 fiber discrimination and origin classification. We investigated the utility of Attenuated  
387 Total **Reflection** (ATR) Fourier Transform Infrared (FTIR) spectroscopy coupled with a  
388 chemometric tool, specifically Partial Least Squares Discriminant Analysis (PLS-DA), for  
389 discriminating various animal hair fibers (cashmere, mohair, yak, camel, alpaca,  
390 vicuña, **llama** and sheep) and differentiating cashmere hair samples from different  
391 origins (Afghanistan, Australia, China, Iran and Mongolia). Scanning Electron  
392 Microscopy (SEM) technique was used to analyze the surface morphology of the  
393 different sample categories.

394 Our findings underscore the effectiveness of ATR-FTIR coupled with PLS-DA in  
395 accurately distinguishing between eight animal hair groups and camelid subgroups.  
396 Specifically, it achieved variance expressions of 99.10 % (18 LVs) and 99.43 % (10 LVs)  
397 when discriminating between eight animal hair groups and camelid subgroups,  
398 respectively. The robustness of our discrimination approach was supported by low  
399 MSECv values, 0.4851 and 0.0437, for eight animal hair groups and camelid  
400 subgroups, respectively.

401 Particularly, ATR-FTIR coupled with PLS-DA effectively classified cashmere hair  
402 samples from different countries, with Mongolian samples demonstrating superior  
403 separation compared to Australian samples, which exhibited higher misclassification  
404 rates. The discrimination seemed to be influenced by the superimposition of alkyl  
405 chain groups of lipids, when detected, and cystine oxides and cysteic acid vibrations  
406 also contributed with a strong influence.

407 Although this study successfully demonstrates the qualitative identification of animal  
408 fibers using PLS-DA, it does not encompass quantitative analysis, which is useful for  
409 blends. Additional research should explore the integration of quantitative methods to  
410 enhance the robustness and applicability of the findings. Moving forward, future  
411 research efforts could focus on addressing some of the limitations encountered in our  
412 study, such as sample size constraints or the exploration of additional discriminant

413 factors beyond amino acid compositions. Additionally, there is potential to further  
414 optimize the ATR-FTIR technique and refine chemometric models to enhance  
415 discrimination accuracy and reliability, as well as investigate other animal hair types,  
416 such as cashmere, whose origins hold significant importance in the fashion industry  
417 and potential susceptibility to commercial frauds.

418 To conclude, our research contributes to advancing the understanding and application  
419 of analytical techniques for discriminating animal hair fibers, taking part in the  
420 preliminary stages of the textile manufacturing process, or as a complementary tool  
421 together with other identification techniques.

422

#### 423 **Author contributions**

424 Conceptualization: Maria Laura Tummino, Vasilios Sakkas; Formal analysis and  
425 investigation: Christoforos Chrimatopoulos, Maria Laura Tummino, Eleftherios Iliadis,  
426 Cinzia Tonetti; Writing - original draft preparation: Christoforos Chrimatopoulos,  
427 Maria Laura Tummino; Writing - review and editing: all the authors; Supervision:  
428 Vasilios Sakkas.

429 **Funding:** The research conducted by Maria Laura Tummino was supported by the  
430 National Research Council of Italy (CNR) in the framework of the Short-Term Mobility  
431 2022 program.

432 **Competing interests:** The authors declare no conflict of interest.

433 **Data Availability:** All data supporting this study are available within the article.

434 **Consent for publication:** The authors agreed with the content and all gave explicit  
435 consent to submit and publish the results presented in the article.

436 **Ethics approval and consent to participate:** This article does not contain any studies  
437 with human participants or animals performed by any of the authors. The authors  
438 claim the compliance with the ethical standards.

439

#### 440 **References**

- 441 1. L. Hunter. "Mohair, Cashmere and Other Animal Hair Fibres". In: R. M.  
442 Kozłowski, M. Mackiewicz-Talarczyk, editors. Handbook of Natural Fibres.  
443 Cambridge, UK: Woodhead Publishing - Elsevier, 2012. Pp. 196–290.  
444 10.1533/9780857095503.1.196.
- 445 2. C. Vineis, C. Tonetti, S. Paoella, P. Pozzo, S. Sforza. "A UPLC/ESI–MS Method for  
446 Identifying Wool, Cashmere and Yak Fibres". Text. Res. J. 2014. 84(9): 953–958.  
447 10.1177/0040517513512394.
- 448 3. W. Lu, J. Fei, J. Yang, M. Tang, Z. Dong, Z. Zhou, et al. "A Novel Method to  
449 Identify Yak Fiber in Textile". Text. Res. J. 2013. 83(8): 773–779.  
450 10.1177/0040517512460301.
- 451 4. "ANNUAL CASHMERE MARKET REPORT 2020". The Schneider Group. 2020.  
452 <https://www.gsneider.com/annual-cashmere-market-report-2020/>  
453 [accessed: Jan 23 2024].
- 454 5. L. Meraviglia. "Technology and Counterfeiting in the Fashion Industry: Friends  
455 or Foes?" Bus. Horiz. 2018. 61(3): 467–475. 10.1016/j.bushor.2018.01.013.
- 456 6. T.J. Lopes, G.R. Rosa, L.S. da Silva, C.W. Scheeren, F.S. Antelo, M.L. Martins.  
457 "Identification, Characterization and Quality Management of Natural Textile  
458 Fibres". In: Md. Ibrahim, H. Mondal, editors. Fundamentals of Natural Fibres  
459 and Textiles. Cambridge, UK: Woodhead Publishing - Elsevier, 2021. Pp. 473–  
460 513. 10.1016/B978-0-12-821483-1.00008-5.
- 461 7. W. Xing, Y. Liu, N. Deng, B. Xin, W. Wang, Y. Chen. "Automatic Identification of  
462 Cashmere and Wool fibers Based on the Morphological Features Analysis".  
463 Micron. 2020. 128: 102768. 10.1016/j.micron.2019.102768.
- 464 8. Y. Zhu, R. Liu, G. Hu, X. Chen, W. Li. "Accurate Identification of Cashmere and  
465 Wool Fibers Based on Enhanced ShuffleNetV2 and Transfer Learning". J. Big  
466 Data. 2023. 10(1): 152. 10.1186/s40537-023-00830-4.
- 467 9. J. Luo, K. Lu, Y. Chen, B. Zhang. "Automatic Identification of Cashmere and Wool  
468 Fibers Based on Microscopic Visual Features and Residual Network Model".  
469 Micron. 2021. 143: 103023. 10.1016/j.micron.2021.103023.

- 470 10. K. Yildiz. "Identification of Wool and Mohair Fibres with Texture Feature  
471 Extraction and Deep Learning". *IET Image Process.* 2020. 14(2): 348–353.  
472 10.1049/iet-ipr.2019.0907.
- 473 11. M. Valentino, J. Behal, C. Tonetti, R.A. Carletto, S. Itri, P. Memmolo, et al.  
474 "Discernment of Textile Fibers by Polarization-Sensitive Digital Holographic  
475 Microscope and Machine Learning". *Opt. Lasers Eng.* 2024. 181: 108395.  
476 10.1016/j.optlaseng.2024.108395.
- 477 12. C. Tonetti, A. Varesano, C. Vineis, G. Mazzuchetti. "Differential Scanning  
478 Calorimetry for the Identification of Animal Hair Fibres". *J. Therm. Anal.  
479 Calorim.* 2015. 119(2): 1445–1451. 10.1007/s10973-014-4247-8.
- 480 13. R. Kumar, D.B. Shakyawar, P.K. Pareek, A.S.M. Raja, L.L.L. Prince, S. Kumar, et  
481 al. "Development of PCR-Based Technique for Detection of Purity of Pashmina  
482 Fiber from Textile Materials". *Appl. Biochem. Biotechnol.* 2015. 175(8): 3856–  
483 3862. 10.1007/s12010-015-1552-z.
- 484 14. "ISO 20418-1:2018 - Textiles — Qualitative and Quantitative Proteomic Analysis  
485 of Some Animal Hair Fibres — Part 1: Peptide Detection using LC-ESI-MS with  
486 Protein Reduction." <https://www.iso.org/standard/67945.html> [accessed: Jan  
487 23 2024].
- 488 15. C. Vineis, C. Tonetti, D.O. Sanchez Ramirez, R.A. Carletto, A. Varesano.  
489 "Validation of UPLC/ESI-MS Method used for the Identification and  
490 Quantification of Wool, Cashmere and Yak Fibres". *J. Text. Inst.* 2017. 108(12):  
491 2180–2183. 10.1080/00405000.2017.1317225.
- 492 16. C. Azémard, E. Dufour, A. Zazzo, J.C. Wheeler, N. Goepfert, A. Marie, et al.  
493 "Untangling the Fibre Ball: Proteomic Characterization of South American  
494 Camelid Hair Fibres by Untargeted Multivariate Analysis and Molecular  
495 Networking". *J. Proteomics.* 2021. 231: 104040. 10.1016/j.jprot.2020.104040.
- 496 17. J. Zhou, R. Wang, X. Wu, B. Xu. "Fiber-Content Measurement of Wool–  
497 Cashmere Blends Using Near-Infrared Spectroscopy". *Appl. Spectrosc.* 2017.  
498 71(10): 2367–2376. 10.1177/0003702817713480.

- 499 18. A. Aljannahi, R.A. Alblooshi, R.H. Alremeithi, I. Karamitsos, N.A. Ahli, A.M. Askar,  
500 et al. "Forensic Analysis of Textile Synthetic Fibers Using a FT-IR Spectroscopy  
501 Approach". *Molecules*. 2022. 27(13): 4281. 10.3390/molecules27134281.
- 502 19. H. Chen, Z. Lin, C. Tan. "Classification of Different Animal Fibers by Near Infrared  
503 Spectroscopy and Chemometric Models". *Microchem. J.* 2019. 144: 489–494.  
504 10.1016/j.microc.2018.10.011.
- 505 20. H. Chen, C. Tan, Z. Lin. "Quantitative Determination of Wool in Textile by Near-  
506 Infrared Spectroscopy and Multivariate Models". *Spectrochim. Acta Part A Mol.*  
507 *Biomol. Spectrosc.* 2018. 201: 229–235. 10.1016/j.saa.2018.05.010.
- 508 21. D. Quintero Balbas, G. Lanterna, C. Cirrincione, R. Fontana, J. Striova. "Non-  
509 Invasive Identification of Textile Fibres using Near-Infrared Fibre Optics  
510 Reflectance Spectroscopy and Multivariate Classification Techniques". *Eur.*  
511 *Phys. J. Plus*. 2022. 137(1): 85. 10.1140/epjp/s13360-021-02267-1.
- 512 22. P. Peets, I. Leito, J. Pelt, S. Vahur. "Identification and Classification of Textile  
513 Fibres using ATR-FT-IR Spectroscopy with Chemometric Methods".  
514 *Spectrochim. Acta - Part A Mol. Biomol. Spectrosc.* 2017. 173: 175–181.  
515 10.1016/j.saa.2016.09.007.
- 516 23. W. Xu, J. Xia, S. Min, Y. Xiong. "Fourier Transform Infrared Spectroscopy and  
517 Chemometrics for the Discrimination of Animal Fur Types". *Spectrochim. Acta*  
518 *Part A Mol. Biomol. Spectrosc.* 2022. 274: 121034. 10.1016/j.saa.2022.121034.
- 519 24. M. Quispe, J.D. Trigo, L. Serrano-Arriezu, J. Huere, E. Quispe, M. Beruete.  
520 "Classification of South American Camelid and Goat Fiber Samples Based on  
521 Fourier Transform Infrared Spectroscopy and Machine Learning". *J. Text. Inst.*  
522 2024. 1–10. 10.1080/00405000.2024.2324209.
- 523 25. B. Barros, C. Rodrigues, S. Sousa, E. Nunes. "Implementation of a Quality Cost  
524 Management Model: Case Study from the Textile Industry Sector". In: E. Alfnes,  
525 A. Romsdal, J.O. Strandhagen, G. von Cieminski, D. Romero, editors. *Advances*  
526 *in Production Management Systems. Production Management Systems for*  
527 *Responsible Manufacturing, Service, and Logistics Futures*. Cham, Switzerland:

- 528 Springer, 2023. Pp. 287–301. 10.1007/978-3-031-43670-3\_20.
- 529 26. M. Rehan Yasin, B. M Nasir, S. Asad Ali Zaidi. “A Case Study in the Textile  
530 Industry for the Reduction of Cost of Quality”. *J. Adv. Technol. Eng. Res.* 2019.  
531 5(6). 10.20474/jater-5.6.1.
- 532 27. I. Cruz-Maya, V. Guarino, A. Almaguer-Flores, M.A. Alvarez-Perez, A. Varesano,  
533 C. Vineis. “Highly Polydisperse Keratin Rich Nanofibers: Scaffold Design and in  
534 vitro Characterization”. *J. Biomed. Mater. Res. - Part A.* 2019. 107(8): 1803–  
535 1813. 10.1002/jbm.a.36699.
- 536 28. J. Manheim, K.C. Doty, G. McLaughlin, I.K. Lednev. “Forensic Hair Differentiation  
537 Using Attenuated Total Reflection Fourier Transform Infrared (ATR FT-IR)  
538 Spectroscopy”. *Appl. Spectrosc.* 2016. 70(7): 1109–1117.  
539 10.1177/0003702816652321.
- 540 29. M.L. Tummino, C. Chrimatopoulos, M. Bertolla, C. Tonetti, V. Sakkas.  
541 “Configuration of a Simple Method for Different Polyamides 6.9 Recognition by  
542 ATR-FTIR Analysis Coupled with Chemometrics”. *Polymers (Basel).* 2023.  
543 15(15). 10.3390/polym15153166.
- 544 30. “ISO 17751-2:2023 - Textiles — Quantitative Analysis of Cashmere, Wool, Other  
545 Specialty Animal Fibres and their Blends — Part 2: Scanning electron  
546 microscopy method”. <https://www.iso.org/standard/83596.html> [accessed:  
547 Jan 23 2024].
- 548 31. S. Sharma, A. Gupta, S.M.S. Bin Tuan Chik, C.Y. Gek Kee, P.K. Poddar.  
549 “Dissolution and Characterization of Biofunctional Keratin Particles Extracted  
550 from Chicken Feathers”. *IOP Conf. Ser. Mater. Sci. Eng.* 2017. 191: 012013.  
551 10.1088/1757-899X/191/1/012013.
- 552 32. A. Barth. “Infrared Spectroscopy of Proteins”. *Biochim. Biophys. Acta -*  
553 *Bioenerg.* 2007. 1767(9): 1073–1101. 10.1016/j.bbabi.2007.06.004.
- 554 33. T. Józwiak, U. Filipkowska, P. Marciniak. “Use of Hen Feathers to Remove  
555 Reactive Black 5 and Basic Red 46 from Aqueous Solutions”. *Desalin. Water*  
556 *Treat.* 2021. 232: 129–139. 10.5004/dwt.2021.27513.

- 557 34. O. Belukhina, D. Milasiene, R. Ivanauskas. "Investigation of the Possibilities of  
558 Wool Fiber Surface Modification with Copper Selenide". *Materials (Basel)*.  
559 2021. 14(7): 1648. 10.3390/ma14071648.
- 560 35. B.H. Stuart. *Infrared Spectroscopy: Fundamentals and Applications*. Chichester,  
561 UK: Wiley, 2004. Pp. 71–93, 137–165. 10.1002/0470011149.
- 562 36. A.C. Pina, N. Tancredi, C.O. Ania, A. Amaya. "Stabilisation of Sheep Wool Fibres  
563 under Air Atmosphere: Study of Physicochemical Changes". *Mater. Sci. Eng. B*.  
564 2021. 268: 115115. 10.1016/j.mseb.2021.115115.
- 565 37. Ş. Duman, M. Küçük. "Cryogenic Milling-based Keratin Microparticle Production  
566 from Anatolian Goat Fibers and their Structural, Chemical and Thermal  
567 properties". *Text. Res. J.* 2023. 93(5–6): 1347–1357.  
568 10.1177/00405175221131334.
- 569 38. N.S. Heliopoulos, S.K. Papageorgiou, A. Galeou, E.P. Favvas, F.K. Katsaros, K.  
570 Stamatakis. "Effect of Copper and Copper Alginate Treatment on Wool Fabric.  
571 Study of Textile and Antibacterial Properties". *Surf. Coatings Technol.* 2013.  
572 235: 24–31. 10.1016/j.surfcoat.2013.07.009.
- 573 39. X. Wang, Z. Shi, Q. Zhao, Y. Yun. "Study on the Structure and Properties of  
574 Biofunctional Keratin from Rabbit Hair". *Materials (Basel)*. 2021. 14(2): 1–15.  
575 10.3390/ma14020379.
- 576 40. M. Shanmugavel, J. Nivedha lakshmi, S. Vasantharaj, C. Anu, L.E. Paul, R.P.  
577 Kumar, et al. "Wealth from Waste: Recovery of the Commercially Important  
578 Waxy Ester from Enzymatic Dehaired Sheep Wool". *Biocatal. Agric. Biotechnol.*  
579 2019. 20: 101255. 10.1016/j.bcab.2019.101255.
- 580 41. Z. Dai, J. Deng, L. Ansaloni, S. Janakiram, L. Deng. "Thin-Film-Composite Hollow  
581 Fiber Membranes Containing Amino Acid Salts as Mobile Carriers for CO<sub>2</sub>  
582 Separation". *J. Memb. Sci.* 2019. 578: 61–68. 10.1016/j.memsci.2019.02.023.
- 583 42. B.A. McGregor, X. Liu, X.G. Wang. "Comparisons of the Fourier Transform  
584 Infrared Spectra of Cashmere, Guard hair, Wool and Other Animal Fibres". *J.*  
585 *Text. Inst. Taylor & Francis*, 2018. 109(6): 813–822.



- 586 10.1080/00405000.2017.1372057.
- 587 43. S.G. Giteru, D.H. Ramsey, Y. Hou, L. Cong, A. Mohan, A.E.D.A. Bekhit. "Wool  
588 Keratin as a Novel Alternative Protein: A Comprehensive Review of Extraction,  
589 Purification, Nutrition, Safety, and Food Applications". *Compr. Rev. Food Sci.*  
590 *Food Saf.* 2023. 22(1): 643–687. 10.1111/1541-4337.13087.
- 591 44. M.C. Corfield, A. Robson. "The Amino Acid Composition of Wool". *Biochem. J.*  
592 1955. 59(1): 62–68. 10.1042/bj0590062.
- 593 45. J.M. Cardamone. "Investigating the Microstructure of Keratin Extracted from  
594 Wool: Peptide Sequence (MALDI-TOF/TOF) and Protein Conformation (FTIR)".  
595 *J. Mol. Struct.* 2010. 969(1–3): 97–105. 10.1016/j.molstruc.2010.01.048.
- 596 46. Y.J. Yang, D. Ganbat, P. Aramwit, A. Bucciarelli, J. Chen, C. Migliaresi, et al.  
597 "Processing Keratin from Camel Hair and Cashmere with Ionic Liquids". *Express*  
598 *Polym. Lett.* 2019. 13(2): 97–108. 10.3144/expresspolymlett.2019.10.
- 599 47. M.A. Khosa, J. Wu, A. Ullah. "Chemical Modification, Characterization, and  
600 Application of Chicken Feathers as Novel Biosorbents". *RSC Adv.* 2013. 3(43):  
601 20800–20810. 10.1039/C3RA43787F.
- 602 48. A. Olfa, H. Taoufik, Z. Riadh, M. Slah. "The Valorization Potential of Tannery  
603 Wool Waste in the Textile Industry". *J. Nat. Fibers.* 2023. 20(1).  
604 10.1080/15440478.2022.2146251.
- 605 49. S. Zanini, A. Citterio, G. Leonardi, C. Riccardi. "Characterization of Atmospheric  
606 Pressure Plasma Treated Wool/Cashmere Textiles: Treatment in Nitrogen".  
607 *Appl. Surf. Sci.* 2018. 427: 90–96. 10.1016/j.apsusc.2017.07.280.
- 608 50. S. Zanini, E. Grimoldi, A. Citterio, C. Riccardi. "Characterization of Atmospheric  
609 Pressure Plasma Treated Pure Cashmere and Wool/Cashmere Textiles:  
610 Treatment in Air/Water Vapor Mixture". *Appl. Surf. Sci.* 2015. 349: 235–240.  
611 10.1016/j.apsusc.2015.05.010.
- 612 51. N. Chandwani, P. Dave, V. Jain, S. Nema, S. Mukherjee. "Improving Anti-Felting  
613 Characteristics of Merino Wool Fiber by 2.5 MHz Atmosphere Pressure Air

- 614 Plasma". *J. Phys. Conf. Ser.* 2017. 823: 012010. 10.1088/1742-  
615 6596/823/1/012010.
- 616 52. R. Kehm, T. Baldensperger, J. Raupbach, A. Höhn. "Protein oxidation -  
617 Formation Mechanisms, Detection and Relevance as Biomarkers in Human  
618 Diseases". *Redox Biol.* 2021. 42: 101901. 10.1016/j.redox.2021.101901.
- 619 53. E.L. Guo, R. Katta. "Diet and Hair Loss: Effects of Nutrient Deficiency and  
620 Supplement Use". *Dermatol. Pract. Concept.* 2017. 7(1): 1–10.  
621 10.5826/dpc.0701a01.
- 622 54. E. Fernández, C. Barba, C. Alonso, M. Martí, J.L. Parra, L. Coderch.  
623 "Photodamage Determination of Human Hair". *J. Photochem. Photobiol. B Biol.*  
624 2012. 106: 101–106. 10.1016/j.jphotobiol.2011.10.011.
- 625 55. R. Atav, F. Türkmen. "Investigation of the Dyeing Characteristics of Alpaca  
626 Fibers (Huacaya and Suri) in Comparison with Wool". *Text. Res. J.* 2015. 85(13):  
627 1331–1339. 10.1177/0040517514563727.
- 628 56. D. Waskitho, E. Lukitaningsih, Sudjadi, A. Rohman. "Analysis of Lard in Lipstick  
629 Formulation Using FTIR Spectroscopy and Multivariate Calibration: A  
630 Comparison of Three Extraction Methods". *J. Oleo Sci.* 2016. 65(10): 815–824.  
631 10.5650/jos.ess15294.
- 632 57. B.A. McGregor, D.J. Tucker. "Effects of Nutrition and Origin on the Amino Acid,  
633 Grease, and Suint Composition and Color of Cashmere and Guard hairs". *J. Appl.*  
634 *Polym. Sci.* 2010. 117(1): 409–420. 10.1002/app.31651.
- 635